https://doi.org/10.5194/egusphere-2026-303
Preprint. Discussion started: 2 February 2026

Causal drivers of alpine flood variability from 1300 to 2020 revealed by climate time series analysis

Juan Carlos Peña-Rabadán[1,2], Lothar Schulte[1], Josep Ramon Miró-Cubells[1,2], Enric Casellas-Masana[1,2], Filipe Carvalho[1]

[1]Fluvalps-PaleoRisk Research Group, Department of Geography, University of Barcelona, Barcelona, 08001, Spain
[2]Meteorological Service of Catalonia, Barcelona, 08017, Spain

Correspondence to: Juan Carlos Peña-Rabadán (juancarlos.pena@gencat.cat)

Abstract. Understanding flood variability in the European Alps is critical for risk management, yet causal mechanisms linking climate drivers to floods remain unclear. Previous studies have largely relied on correlations, limiting causal attribution. Here we apply a constraint-based causal inference framework using the PC-stable algorithm, combined with bootstrap stability analysis and Granger causality validation, to multi-centennial climate and flood proxy records from the Hasli-Aare catchment (1300–2020 CE). Our results reveal that total solar irradiance modulates summer atmospheric circulation, notably the summer North Atlantic Oscillation, which causally influences alpine flood frequency. These relationships are strongest during the preindustrial period and weaken under modern anthropogenic forcing, indicating a shift in dominant flood drivers. Our study demonstrates the utility of causal inference methods in paleoclimate research and offers a framework for investigating changes in the drivers of hydrological extremes, important for climate attribution and risk assessment in mountain environments.

1 Introduction

Research on paleofloods conducted by Schulte et al. (2009, 2015, 2019) developed an integrated multi-archive approach to examine the climate drivers of summer flood variability in the Hasli-Aare catchment (46°41′N, 6°04′E; 596 km²) of the Bernese Alps, Switzerland, over the past 700 years (top panel of Fig. 1). This catchment is particularly significant due to its unique geological and climatic characteristics, which render it highly susceptible to floods influenced by both local and regional climate processes. By integrating geochemical proxies extracted from floodplain and lake sediments with historical and botanical flood records, these studies aimed to elucidate climatic mechanisms governing flood frequency and magnitude in this Alpine region. All variables employed in this analysis are comprehensively defined in the Glossary provided in Supplementary Material 1 (Table S1.1), and the Sea Level Pressure grids used in the analysis are described in Table S1.2 of Supplementary Material 1.

Multi-archive studies of Alpine paleofloods (Schulte et al., 2019a, 2019b; see Fig. 1) highlight the need to synthesize diverse proxies to address uncertainties, flood thresholds, asynchronous flood pulses, and contrasting flood trends. This synthesis is essential for understanding the complex interactions between climate drivers and hydrological responses (Schulte et al., 2020; see bottom panel Fig. 1).

https://doi.org/10.5194/egusphere-2026-303
Preprint. Discussion started: 2 February 2026

The present study applies causal inference methods to understand the climate variability driving summer floods in the Bernese Alps. We use the geochemical paleoflood series (Schulte et al., 2019a), which identified eleven major flood pulses (1300-1320, 1390-1400, 1450-1470, 1550-1570, 1590-1610, 1650-1670, 1690-1710, 1715-1735, 1770-1790, 1800-1820, and 1830-1850 CE) and six periods associated with major flood-poor intervals characterized by soil formation processes (1360-1380, 1540-1560, 1640-1660, 1770-1790, 1880-1900, and 1955-1977 CE). Due to the chronological uncertainties of sedimentary records, these pulses are considered within a twenty-year range around their respective peak values (F1 maximum/minimum in Fig. 1, Flood_F1 in this paper). Visual correlations suggest that the three principal negative TSI (Total Solar Irradiance) pulses (A, B, and D; see bottom panel Fig. 1) align with flood pulses, negative Summer North Atlantic Oscillation anomalies (SNAO; Folland et al., 2009; Peña et al., 2015; see Fig. 1.1 and Fig. 1.2 in Supplementary Material 1), lower Northern Hemisphere summer temperatures, decreased Alpine summer temperatures, and reduced Alpine spring precipitation (from dendrochronological reconstructions). The latter is not plotted in the graph (see Schulte et al., 2019 for more information). Both temperature series exhibit similar responses to volcanic forcing, which induces a cooling effect and can modulate the occurrence of flood pulses.

To understand the climatological pattern of these flood pulses in the past, the map related to no-flooding periods (left panel of Fig. S1.3. in the Supplementary Material 1) presents a positive Summer North Atlantic Oscillation (SNAO, Folland et al., 2009; Peña et al., 2015) phase, while the flooding periods (right panel of Fig. S1.3. in Supplementary Material 1) show negative anomalies over Europe, like SNAO negative phase. Furthermore, the SNAO influences the spatial distribution of flood events (Peña et al, 2020). Negative SNAO phases, often associated with low-pressure systems over northern Europe, correlate with heightened flood activity on the northern slopes of the Alps, including the Hasli-Aare catchment. Conversely, positive SNAO phases are linked to intensified Atlantic cyclones in the Mediterranean region that predominantly impact the southern slopes of the Alps, altering precipitation patterns and snowmelt dynamics (Peña et al, 2015, 2020) as also reported by other studies (Hirschi et al., 2006). In this context, our study introduces a comprehensive causal analysis of both external and internal climate drivers associated with historical extreme hydrological events. Although anthropogenic factors such as land-use changes, urbanization, and improved flood monitoring have contributed to the increased frequency and intensity of floods since the late 20th century, our findings indicate that natural climate variability, particularly the SNAO modulated by solar activity (TSI), plays a pivotal role in shaping flood patterns in the Hasli-Aare catchment (Peña et al., 2015, 2020). However, while preliminary visual correlations offer valuable geomorphological and palaeoclimatological insights, it is necessary to validate these findings using robust statistical relationships.

A rigorous assessment of the stability and causality of these associations is necessary to distinguish genuine climatic mechanisms from coincidental correlations. Therefore, this study employs causal inference methodologies to investigate these complex climate-flood relationships. By applying state-of-the-art causal inference methodologies to long-term climate and flood records, we aim to identify the underlying causal pathways linking the climate system to flood events (Fig. 2).

https://doi.org/10.5194/egusphere-2026-303
Preprint. Discussion started: 2 February 2026

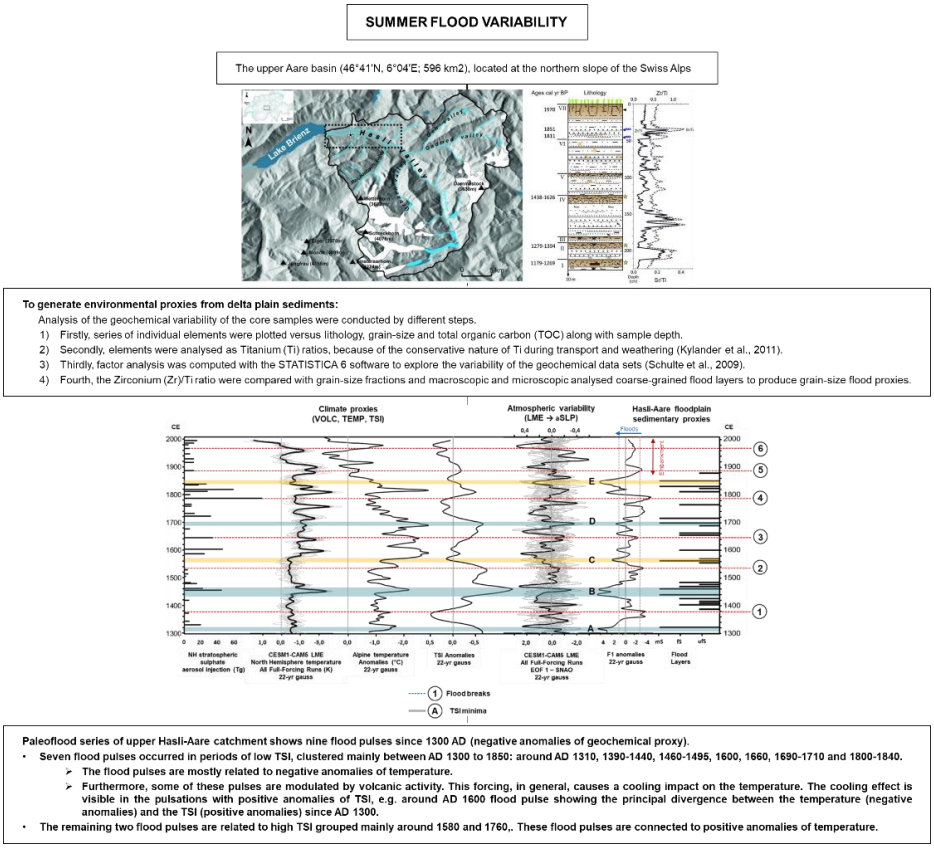

Fig. 1 Location of study area (left top panel): Shaded relief of a digital elevation model (Swisstopo) shows the Hasli-Aare catchment in the Bernese Alps. White areas represent the areas of principal glaciers in the catchment. The star indicates the location of the key-core in the floodplain of the Hasli-Aare River. Key section AA-05 (right top panel): lithology, chronology and Zr/Ti and Sr/Ti ratios of section AA-05. Organic soils are shown in brownish colours. Peaks in these ratios correspond to flood layers. For further details of location, lithology and geochemistry of retrieved cores see Schulte et al. (2015). (Adapted from Peña & Schulte (2020). Bottom panel, right to left: flood layers (coarse-grained flood layers from Hasli delta plain sediments, Schulte et al., 2015), Factor 1 scores of geochemical elements (Schulte et al., 2015), SNAO (Peña et al., 2015), anomalies of TSI (Steinhilber et al., 2009), Alpine temperature anomalies for June-August (Büntgen et al., 2006, 2011), simulated Northern Hemisphere temperature anomalies for July-August (Peña & Schulte, 2020: CESM-LME data), and stratospheric sulphate aerosols for the Northern Hemisphere (Gao et al., 2008). Flood breaks (red dashed lines) indicate the end of major flood periods and correspond to land surface stability episodes. Principal flood pulses are marked by light blue (negative TSI/temperature anomalies) or yellow (positive TSI/temperature anomalies).

https://doi.org/10.5194/egusphere-2026-303
Preprint. Discussion started: 2 February 2026

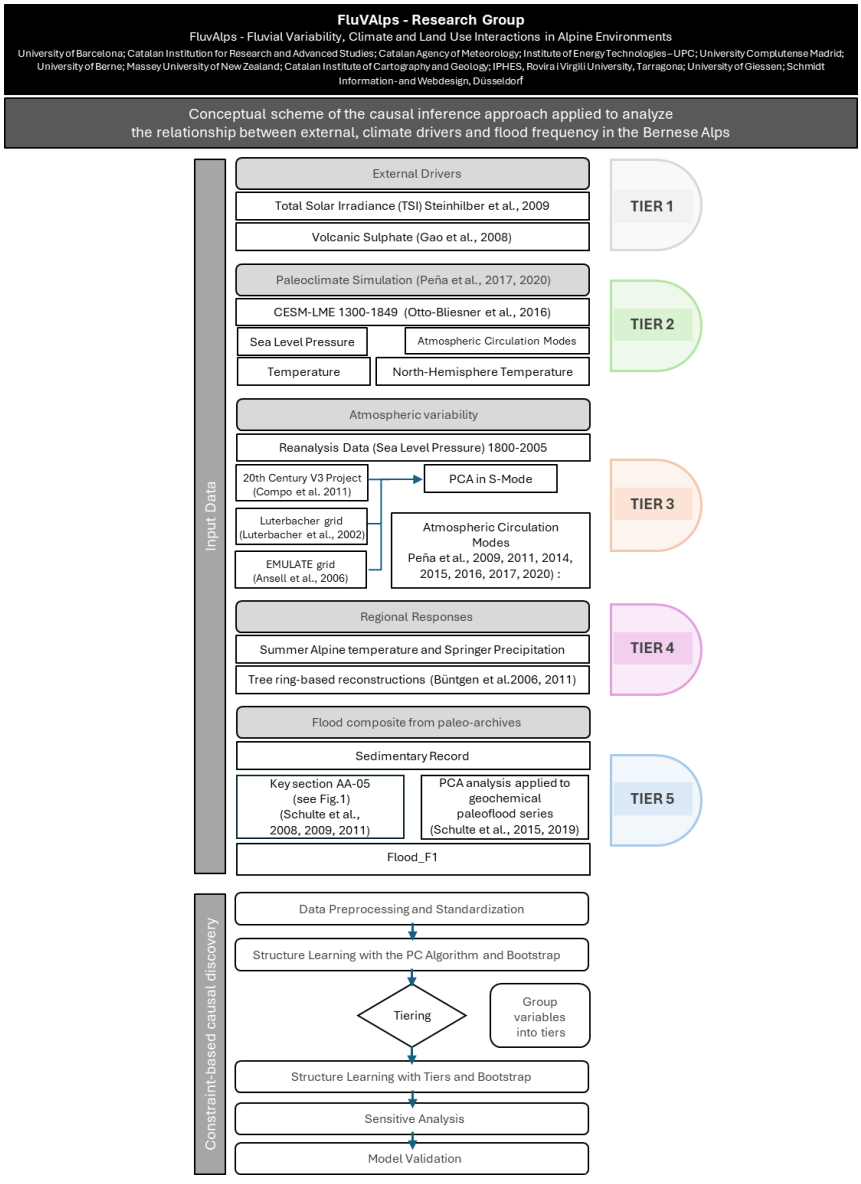

Fig. 2 Conceptual scheme of the causal inference approach applied to analyze the relationship between climate variability and flood frequency in the Bernese Alps. The figure illustrates the integration of historical and paleoclimatic data, including sea level pressure (SLP) datasets, total solar irradiance (TSI), volcanic sulphate, northern-hemispheric temperature and Alpine temperature/precipitation, into a Bayesian network. Principal Component Analysis (PCA) is used to identify key atmospheric circulation patterns, such as the Summer North Atlantic Oscillation (SNAO), which are subsequently incorporated into a causal model based on Directed Acyclic Graphs (DAGs). The PC-algorithm enables the identification of causal dependencies while addressing confounding variables. This comprehensive approach combines simulated and reconstructed climate data to investigate flood variability (Flood_F1) and assess the robustness of causal relationships, highlighting the influence of large-scale climate and regional drivers on hydrological extremes. References include the previous research of the Fluvalps-PaleoRisk Research Group (http://palaeo.org/) in the period 2008-2025 (e.g., Schulte et al., 2008, 2009, 2011, 2015, 2019; Peña et al., 2009, 2011, 2014, 2015, 2016, 2017, 2020).

https://doi.org/10.5194/egusphere-2026-303
Preprint. Discussion started: 2 February 2026

2 Data Preprocessing and Standardization

The datasets used in our analysis are shown in Table S1.1 and Table S2.1. in the Supplementary Material 1, with original references provided. To account for dating uncertainties in paleoclimate proxies, we cannot rely on a single year for causal inference. We therefore use a ±20-year window around each target year, sampling each year 100 times with a Monte Carlo simulation (ages drawn uniformly within ±20 years of the nominal date). This interval is based on prior work (Schulte et al., 2015), which demonstrated that a ±20-year window adequately captures typical sedimentary dating uncertainty. Sensitivity tests with narrower (±10) and wider (±30) windows confirmed that ±20 years provides a reasonable balance between capturing real variability and maintaining model robustness.

The data are divided into two periods: pre-industrial (1300–1849 CE) and industrial (1850–2005 CE), encompassing the anthropogenic warming era. This split allows us to test whether causal relationships remain stable under different climate regimes. All variables were standardized (subtracting the mean and dividing by the standard deviation) to ensure comparability and to meet the assumptions of correlation-based conditional independence tests.

3 Methods

3.1 Analytical Framework

We use a structured, multi-phase approach combining data-driven discovery with physical constraints. Our framework includes:

- Granger Causality Analysis to identify temporal precedence (Sect. 3.2).
- Conditional Independence Testing (PC-stable algorithm) to screen for potential causal links (Sect. 3.3).
  - Bayesian Network Structure Learning (using the bnlearn R package, Scutari 2010) to infer directed relationships.
  - Bootstrapping (100 iterations) to assess edge stability.
- Domain Constraints via a tiered blacklist to enforce physical plausibility (Sect. 3.4).
- Sensitivity Analysis and Model Validation, including cross-epoch comparison, out-of-sample log-likelihood, and structural stability checks (Sect. 3.5).

3.2 Granger Causality Analysis

Granger causality (Granger, 1969) tests whether past values of one time series statistically improve prediction of another (see also Supplementary Material 2) . While not proof of true causality, it provides a test of temporal precedence. We performed pairwise Granger tests with lag selection by the Bayesian Information Criterion (BIC), using characteristic lag times for

https://doi.org/10.5194/egusphere-2026-303
Preprint. Discussion started: 2 February 2026

forcings and circulation indices (Table S2.1 in Supplementary Material 2). These results serve as an external check on the links inferred by the PC algorithm.

3.3 Structure Learning with the PC Algorithm and Bootstrapping

In climate science, a Directed Acyclic Graph (DAG) can represent a Bayesian Network that helps model the complex, probabilistic dependencies between variables that influence climate patterns over time, accounting for causal relationships. The DAG represents key climate indices or factors, while the edges represent conditional dependencies, indicating potential causal relationships. The network allows us to infer the probabilistic influence of various climate factors on each other. Graphical representations (via strength plots and average networks) then illustrate which causal relationships are most stable. This study employs the Peter-Clark algorithm (PC) to infer causal structure between climate variables and flood variability (see complete description of methodology in Supplementary Material 3). The methodology follows a multi-step approach to ensure robustness and consistency across different climate periods, including flood variability (F1_Flood), atmospheric circulation indices, temperature, precipitation, and external forcings (solar and volcanic activity). The algorithm follows these steps:

- Edge Selection: Start with a fully connected graph, then remove edges that become conditionally independent given any subset of other variables.
- Edge Orientation: Assign arrow directions using collider patterns and logical constraints, ensuring a directed acyclic graph.
- Bootstrap Validation: Repeat the structure learning 100 times on resampled datasets (including ±20-year perturbations) to compute edge stability (occurrence frequency)(Xiang et al., 2023).

We selected significance thresholds for edge inclusion based on these bootstrap frequencies. Specifically, by running PC with dating uncertainty perturbations, we derive statistical consistency thresholds: only edges with stability above these thresholds are retained.

3.4 Incorporating Domain Constraints in Causal inference

To ensure physical plausibility, we organized variables into a tiered hierarchy reflecting causal order: external forcings (top tier), large-scale climate drivers, atmospheric modes, regional responses, and finally observed hydrological impacts (bottom tier). We applied a blacklist to forbid edges that violate this ordering (e.g., no feedback from floods to solar forcing). This constraint prevents the algorithm from assigning causality in the absence of a plausible mechanism. By enforcing this hierarchy, the final DAG aligns with known climate processes, reduces spurious links, and improves interpretability (Spirtes et al., 2000; Peters et al., 2017).

The tiered architecture and use of blacklists together serve as a form of soft expert knowledge integration, which has been shown to improve the robustness and realism of causal inference in Earth system sciences (Runge et al., 2019; Kretschmer et al., 2021).

https://doi.org/10.5194/egusphere-2026-303
Preprint. Discussion started: 2 February 2026

3.5 Sensitivity Analysis and Model Validation

We tested robustness in several ways. First, we conducted split-sample validation by training DAGs on pre-industrial data (1300–1849 CE; Section 4.3) and testing on industrial data (1850–2005 CE). Second, we evaluated out-of-sample log-likelihoods: for each period, we computed the log-likelihood of data under the DAG trained on the other period. A substantial drop in likelihood when applied to the industrial data would indicate structural changes due to anthropogenic influence. Third, we examined structural stability by comparing key edges across the two periods, identifying which links persist or change under climate shifts.

4 Results

4.1 Causal inference Framework Performance

Our PC-stable causal-inference framework successfully uncovers plausible and stable links among solar, atmospheric, and hydrological variables. The method relies on conditional independence testing (not just pairwise correlations) to build the network skeleton; directionality comes from collider patterns and logical rules, and edge stability is assessed via bootstrapping. Similar constraint-based methods have been applied in Earth-system climate studies (Runge et al., 2019; Kretschmer et al., 2016). Unlike mutual-information or Granger-only approaches, PC focuses on conditional structure, which helps separate direct from indirect effects.

4.2 Granger Causality Testing

As an independent check, we applied pairwise Granger-causality tests (complete results in Supplementary Material 2) to selected node pairs (e.g., TSI → EOF1, EOF1 → Flood_F1) using a vector-autoregressive model with lag selection (BIC). While a significant Granger result does not prove causality, it indicates temporal precedence. We found several relationships with $p \leq 0.10$ (Table 1), reinforcing the links detected by the PC-stable algorithm.

Table 1: Granger Causality Results (Full table in Supplementary Material 2.)

Predictor	Target	p_value
TSI	EOF1	0.095
	Pamj_Alps	0.007
NH_Volcanic	NH_Tja	0.099
	Tjja_Alps	<0.001
	Pamj_Alps	0.077
	Flood_F1	0.079
EOF1	Tjja_Alps	0.033
	Pamj_Alps	0.079
	Flood_F1	0.097
NH_Tja	Tjja_Alps	0.025
	Pamj_Alps	<0.001
	Flood_F1	0.051

https://doi.org/10.5194/egusphere-2026-303
Preprint. Discussion started: 2 February 2026

Pamj_Alps	Flood_F1	<0.001

4.3 Structure Learning with the PC Algorithm and Bootstrapping

Using the PC algorithm with 100 bootstrap iterations, we constructed a robust DAG of conditional dependencies. Edge stability is quantified as the frequency of each edge appearing across bootstraps. We set a significance threshold of 0.58 to identify highly stable edges (depicted in Fig. 3; more information: Fig. S3.1., Table S3.1 in supplementary Material 3).

The resulting DAG captures the main climatic drivers of flood variability in the Hasli-Aare catchment. It shows coherent links among variables; however, there was a weak or inconsistent link between the flood proxy (Flood_F1) and Alpine precipitation (Pamj_Alps). To impose physical realism, we applied the tiered constraints described above, yielding a constrained DAG consistent with established climate dynamics (e.g., Hurrell et al., 2003).

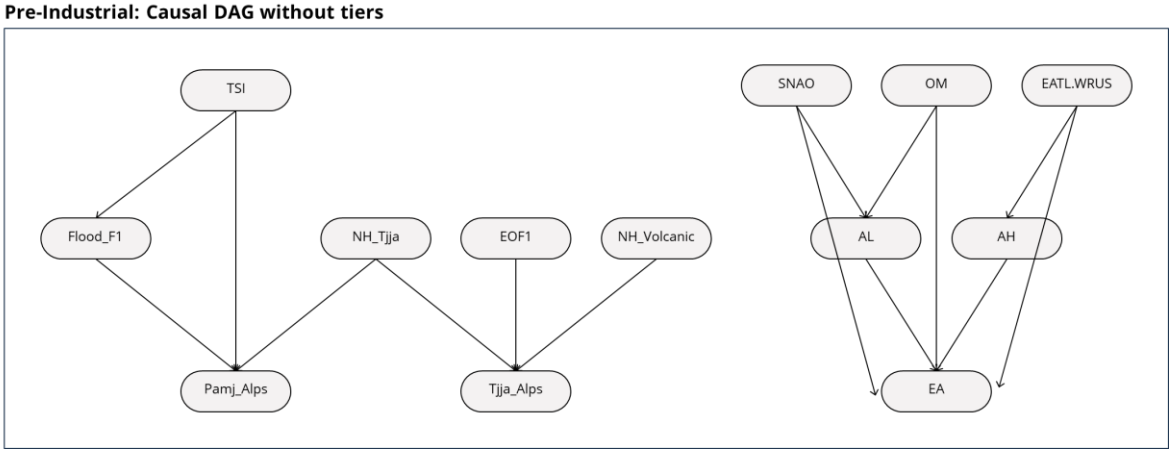

Fig. 3. Unconstrained DAG for pre-industrial period (edges with >58% bootstrap confidence). Major variables: TSI, atmospheric PCs (EOFs), Alpine temperature (Tjja_Alps), Alpine precipitation (Pamj_Alps), volcanic forcing, and flood index (Flood_F1).

4.4 Key Findings from the Constrained DAG

To incorporate physical plausibility into the causal inference process, we applied expert-defined blacklists to exclude nonphysical edges, such as feedback links from internal climate or hydrological variables to external forcings. This constraint ensured that the resulting DAG respected established cause–effect relationships in the climate system. By guiding the algorithm with physically informed rules, the constrained model avoided spurious associations and yielded more interpretable causal structures.

The constrained DAG resulted in a lower significance threshold for edge retention (0.41; Fig. S3.2. and Table S3.2, in Supplementary Material 3), while preserving key structural components of the unconstrained network. A visual comparison of the unconstrained (Fig. 3) and constrained DAGs (Fig. S3.3. in Supplementary Material 3) highlights how the integration of physical knowledge alters the inferred network topology and strengthens interpretability.

The constrained DAG yields the following direct causal links (Fig. 4):

https://doi.org/10.5194/egusphere-2026-303
Preprint. Discussion started: 2 February 2026

- TSI → EOF1: Total solar irradiance drives the leading mode of atmospheric variability (EOF1), aligning with the influence of solar cycles on large-scale circulation.
- TSI → Flood_F1: TSI is causally linked to flood variability in the Bernese Alps, supporting hypotheses that solar activity modulates hydrological extremes in high-altitude regions.
- TSI → Pamj_Alps: TSI influences precipitation variability in the Alpine region (from tree-ring reconstructions), reinforcing the solar imprint on regional hydroclimate.
- EOF1 → Pamj_Alps: Large-scale atmospheric variability modulates Alpine summer precipitation, likely via shifts in storm tracks.
- EOF1 → Flood_F1: EOF1 (hemispheric circulation) directly affects flood frequency, consistent with floods resulting from extreme precipitation under certain circulation regimes.
- EOF1 → Tjja_Alps: Atmospheric variability significantly influences Alpine summer temperatures, possibly via changes in air-mass pathways.
- NH_Volcanic → Tjja_Alps: Volcanic forcing is causally linked to summer cooling in the Bernese Alps, reflecting the well-documented temperature response to stratospheric aerosol loading following major eruptions.

4.5 Sensitivity Analysis and Structural Shifts in a Global Warming

To evaluate the generalizability and temporal resilience of the inferred causal network, we conducted a sensitivity analysis comparing DAG structures across the preindustrial (1300–1849 CE) and industrial (1850–2005 CE) periods. This was achieved by computing out-of-sample log-likelihoods based on perturbed datasets with randomized temporal displacements. The average log-likelihood for the industrial era (−2,268; Fig. S3.4. in the Supplementary Material 3) was substantially lower than for the preindustrial period, indicating a degradation in explanatory power and suggesting significant structural evolution in the underlying climate–flood relationships.

Despite this, several key preindustrial pathways remain detectable in the industrial network (Fig. 4; Fig. S3.5. and Fig. S3.6.in Supplementary Material 3). Notably, the robust causal link TSI → EOF1 persists, consistent with long-term solar influence on atmospheric circulation. However, TSI → Pamj_Alps and TSI → Flood_F1 both weaken substantially under industrial conditions, implying that anthropogenic forcing has disrupted these earlier links (Table S3.3 in Supplementary Material 3).

Several structural changes highlight this transition: the causal connection from volcanic forcing to temperature (NH_Volcanic → Tjja_Alps) vanishes, likely because large eruptions have been fewer and greenhouse warming has dominated recent temperature trends. New links appear, for example, TSI → Tjja_Alps (solar affecting Alpine temperature) and links involving the East Atlantic (EA) circulation index, suggesting a reorganization of teleconnections under altered boundary conditions. Perhaps most strikingly, some flood-related edges present pre-industrially disappear entirely in the industrial DAG. This suggests flood variability has become more decoupled from natural modes, consistent with a rising anthropogenic signal in extreme hydrology.

https://doi.org/10.5194/egusphere-2026-303
Preprint. Discussion started: 2 February 2026

Nevertheless, certain core relationships endure across both periods. Northern Hemisphere summer temperature anomalies (NH_Tja) continue to influence Alpine summer temperature (Tjja_Alps), and the SNAO continues to modulate the EA pattern. These persistent edges indicate that some fundamental thermodynamic linkages persist even as the climate system evolves.

Our results reveal a non-stationary causal structure in the climate–flood system under anthropogenic forcing. They highlight the limitations of applying pre-industrial climate–flood models to the modern era without accounting for emergent human influences. They emphasize the need for time-explicit causal inference to separate enduring physical mechanisms from those altered by climate change.

The stability—or disruption—of causal relationships among key climate variables between the pre-industrial and industrial periods reveals fundamental structural changes in the climate system, likely driven by anthropogenic influences.

Our analysis of edge stability under dating uncertainty highlights several significant shifts in causal pathways. One of the most robust and persistent links is the association between TSI and EOF1, which remains stable across both periods. This enduring connection reinforces the pivotal role of solar variability in modulating atmospheric circulation over long timescales. However, during the industrial period, TSI no longer exhibits strong causal links with precipitation or flood timing, suggesting that human-induced forcings may have supplanted or masked natural drivers in regulating hydrological extremes. Also, new causal pathways emerge in the industrial period, including associations between TSI and temperature reconstructions, as well as with the East Atlantic (EA) pattern. These novel connections indicate a reorganization of the climate system's internal dynamics in response to external forcings. In particular, the breakdown of historical TSI → Pamj_Alps linkages and the emergence of TSI → EA interactions point toward anthropogenically driven modifications in the way energy is distributed within the climate system.

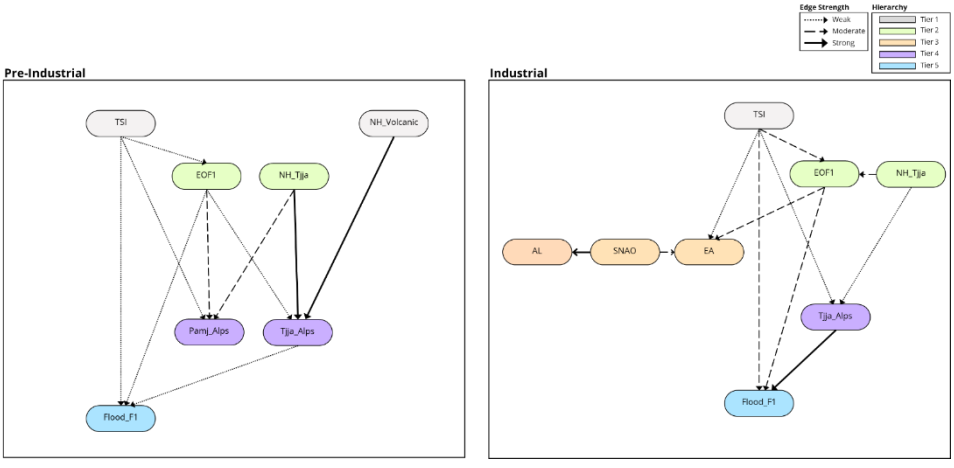

Fig. 4 Comparison of constrained network structures for the pre-industrial (a) and industrial (b) periods. Node colours indicate variable groups (solar, atmospheric, hydrological), and edge widths represent bootstrap stability. The diagram highlights the persistence of the TSI → EOF1 link across both eras and the weakening of TSI → Pamj_Alps and TSI → Flood_F1 in the industrial period. New industrial-era links (e.g., between TSI and Alpine temperature, or with the East Atlantic pattern) indicate a reorganization of the climate system under anthropogenic influence. The breakdown of historical TSI → precipitation ties and emergence of TSI → EA pathways suggest that human forcings have modified how solar variability affects regional hydroclimate. (See Discussion §5.1 for interpretation)

https://doi.org/10.5194/egusphere-2026-303
Preprint. Discussion started: 2 February 2026

Collectively, these results imply that the emerging TSI → EA interaction in our industrial-era DAG is not a residual preindustrial feature, but rather a reorganization of atmospheric pathways under changing radiative boundary conditions. This underscores the need for causality-based frameworks that account for temporal nonstationary in evaluating both natural and anthropogenically driven climate linkages.

One of the results is the weakening and, in some cases, the disappearance, of previously stable causal edges. For example, links such as EOF1 → Tjja_Alps, EOF1 → Pamj_Alps, and Tjja_Alps → Pamj_Alps, robust in the pre-industrial era, are absent or weakened in the industrial period (Table S3.3. in Supplementary Material 3). The lack of a consistent connection between volcanic activity and reconstructed temperature in the industrial period reflects both the reduced frequency of major eruptions in recent decades.

However, the disappearance of several key relationships—particularly those involving precipitation and flood timing—underscores the limitations of applying pre-industrial climate models to modern contexts without accounting for structural shifts. Relying on outdated causal frameworks may lead to inaccurate attributions and projections, particularly concerning regional hydroclimatic variability.

Taken together, our findings underscore the importance of distinguishing between natural and anthropogenically modified causal pathways when analysing climate dynamics. The inability of the pre-industrial DAG to fully explain modern climate interactions highlights the need for temporally adaptive analytical frameworks. Recognizing these evolving causal structures is essential for improving climate model fidelity, enhancing attribution studies, and advancing our understanding of Earth's increasingly complex and human-influenced climate system. The multidimensional approach captures the complexity of the climate system, offering insight into long-term interactions between climate variability and flood dynamics in Alpine environments.

5 Discussion and Implications

Our causal inference framework, based on the PC-stable algorithm implemented in the bnlearn R package, identifies statistically robust and directionally consistent dependencies between external and internal forcings with extreme hydrological responses in the Hasli catchment. Importantly, the algorithm does not estimate causal effects through conditional probabilities or t-statistics. Instead, it relies on conditional independence testing via partial correlations, constructing a causal graph by identifying the minimal set of statistically supported dependencies. Edge directions are then inferred through v-structure analysis and orientation rules that preserve the acyclic property of Bayesian networks. To ensure the stability of inferred links, we employ bootstrapping with temporal perturbations, capturing the robustness of the causal structure under observational uncertainty.

This constraint-based approach has been increasingly adopted in Earth system science, offering a formal framework to disentangle complex dependencies in climatic systems. For instance, Runge et al. (2019) applied causal network methods to detect directed dependencies in global climate fields, while Kretschmer et al. (2016) used similar techniques to identify

https://doi.org/10.5194/egusphere-2026-303
Preprint. Discussion started: 2 February 2026

causality between Arctic sea ice variability and mid-latitude atmospheric circulation. Unlike Granger causality or mutual information–based techniques, which often reflect average or lagged associations, the PC-stable method emphasizes local conditional independence, providing a clearer picture of plausible underlying mechanisms.

Our findings reinforce emerging evidence that natural solar variability can modulate regional hydroclimatic extremes through atmospheric teleconnections. Similar hypotheses have been explored in paleoclimate and historical hydrology studies, where solar-induced shifts in atmospheric modes, such as the SNAO, have been linked to increased flood frequency or severity across Europe (Knudsen et al., 2009; Martín-Chivelet et al., 2011, Peña & Schulte, 2020). Furthermore, recent modelling studies have also demonstrated the potential influence of total solar irradiance (TSI) variations on multidecadal hydroclimatic variability (Zanchettin et al., 2008, Schulte et al., 2015, Lean et al., 2022). By integrating these insights within a data-driven, causality-focused framework, our analysis offers novel support for the role of solar-atmospheric mode coupling in shaping flood hazard dynamics over centennial timescales. Recent studies highlight the potential of causal inference in the analysis of Earth System Science. Su et al. (2023) underline how causal inference methods are reshaping the Earth System Science paradigm by integrating mechanism-driven models with data-driven methods. This integration enhances the ability to reveal concealed causal connections in complex systems. Similarly, Runge et al. (2019) emphasize the potential of causal network analysis in handling spatiotemporal data. Finally, the study by Silini et al. (2023) demonstrates the utility of causal inference in identifying causal links among climatic indices like NAO and ENSO.

Our study employs causal inference to unravel the complex interactions between external forcings, climate variability, and flood risk in the Bernese Alps, emphasizing how diverse global and regional climate factors influence flood variability. Utilizing Bayesian network methods, specifically the PC algorithm, the research maps conditional probabilities across causal pathways, tracing the progression from broad climate drivers to specific flood outcomes (Pearl, 2000; Spirtes et al., 2000).

5.1 Broad Climate Drivers as Baseline Modulators of Flood Risk

The constrained DAG uncovers a coherent set of causal pathways linking external forcings, large-scale atmospheric variability, and regional hydroclimatic responses in the Bernese Alps. Our analysis reaffirms the pivotal role of TSI as a driver of atmospheric and hydrological variability, a relationship increasingly recognized in studies of Holocene climate dynamics (Steinhilber et al., 2009; Wu et al., 2018). The robust causal link between TSI and the principal mode of summer atmospheric circulation is consistent with mechanisms proposed by Gray et al. (2010), wherein solar UV variability modulates stratosphere–troposphere coupling, potentially amplifying SNAO-like patterns. This dynamical pathway has also been supported by climate model experiments linking solar forcing to shifts in mid-latitude circulation (Ineson et al., 2011; Scaife et al., 2013).

Through this pathway, changes in TSI are transmitted to regional precipitation and flood regimes during the preindustrial period: the direct links TSI → Pamj_Alps and TSI → Flood_F1 imply that solar forcing exerts a detectable influence on Alpine hydroclimate extremes in that era, consistent with tree-ring reconstructions that capture solar-driven moisture anomalies (Büntgen et al., 2011). This cascade effect is particularly pronounced during periods of low solar activity in the preindustrial

https://doi.org/10.5194/egusphere-2026-303
Preprint. Discussion started: 2 February 2026

era, which our results associate with heightened flood risk, a finding consistent with paleoclimate records from the Alps (Wirth et al., 2013; Schulte et al., 2015; Büntgen et al., 2021).

The detected NH_Volcanic → Tjja_Alps link further validates the well-established cooling effect of stratospheric aerosols on regional summer temperatures (Robock, 2000; Schneider et al., 2009). This result demonstrates that our constrained causal framework not only captures solar-driven variability but also volcanic forcing, thereby offering a unified representation of natural external drivers. Volcanic forcing exhibited weaker direct links to flood variability, despite its known capacity to perturb hemispheric temperatures (Sigl et al., 2015; Stoffel et al., 2015). This discrepancy may reflect the transient nature of volcanic aerosol impacts, which are often dampened in sediment archives due to proxy smoothing effects (Toohey et al., 2017). However, the strong Granger-causal relationship between volcanic aerosols and Alpine temperatures underscores the potential for episodic eruptions to disrupt regional hydroclimatic stability, as observed following the 1815 Tambora eruption (Brönnimann et al., 2019; Schulte et al., 2019).

Finally, recent causal inference studies (e.g., Carvalho-Oliveira et al., 2024) have demonstrated that North Atlantic extratropical sea surface temperatures (potentially influenced by long-term solar variability), modulate the predictability and dynamics of the EA pattern, reinforcing the physical plausibility of a TSI–EA teleconnection. Concurrently, modelling efforts and reconstructions (e.g., Ruprich-Robert & Cassou, 2015; Neukom et al., 2018) indicate that the influence of the EA pattern on multidecadal climate variability has intensified under greenhouse gas forcing, particularly in relation to Atlantic sector hydroclimate. These findings are further supported by process-based paleoclimate reconstructions, which suggest that solar-forced variability has historically projected onto EA-like modes of circulation, though its imprint has weakened in the presence of dominant anthropogenic signals (e.g., Ljungqvist et al., 2019). Collectively, these results imply that the emerging TSI → EA interaction in our industrial-era DAG is not a residual preindustrial feature, but rather a reorganization of atmospheric pathways under changing radiative boundary conditions. This underscores the need for causality-based frameworks that account for temporal nonstationary in evaluating both natural and anthropogenically driven climate linkages.

5.2 Intermediate Climate Patterns: Bridging Global Forcings and Regional Responses

The role of EOF1 as an intermediary (via EOF1 → Pamj_Alps and EOF1 → Flood_F1) highlights the importance of large-scale circulation shifts in focusing preconditioning and triggering of extreme rainfall events. This finding supports physical mechanisms by which a positive summer NAO phase or equivalent circulation anomaly promotes southward storm trajectories into the Alps, enhancing orographic uplift and precipitation intensity (Luterbacher et al., 2006). Moreover, the causal link EOF1 → Tjja_Alps underscores how circulation anomalies translate into thermal anomalies through altered advection of air masses, reinforcing the tight coupling between precipitation and temperature regimes in mountainous terrain.

Our finding (Schulte et al., 2015; Peña & Schulte, 2020) that negative/positive SNAO phases enhance flood risk mirrors modern observational studies (Folland et al., 2009; Horton et al., 2009) but extends this relationship to centennial timescales. Notably, the SNAO's coupling with TSI anomalies suggests that solar minima may be associated with blocking patterns over

https://doi.org/10.5194/egusphere-2026-303
Preprint. Discussion started: 2 February 2026

Scandinavia, a mechanism previously hypothesized for the Little Ice Age (Moffa-Sánchez et al., 2019) and now statistically supported through causal networks.

This bridging role of the SNAO highlights the importance of atmospheric tele-connections in mediating global-to-regional climate impacts. Similar linkages have been documented in the Himalayas, where the Indian Summer Monsoon serves as an analogous intermediary between tropical SSTs and flood regimes (Shi et al., 2022). Our work thus contributes to a growing consensus that intermediate circulation modes are amplifiers of mountain hydrology (IPCC, 2021; Viviroli et al., 2020). Understanding the interactions among solar irradiance, SNAO, and other climate indices is essential for advancing flood risk models and crafting robust adaptation strategies for alpine regions.

5.3 Direct Flood Triggers: Temperature and Precipitation Extremes

The finding of the strength of temperature and precipitation edges on the variability of floods (modulated by solar activity and atmospheric modes) is corroborated by several studies.

The dual role of temperature anomalies—amplifying snowmelt during warm phases and prolonging soil saturation during cold phases—reveals a nuanced relationship between warming and flood risk (Schulte et al., 2015). While anthropogenic warming is projected to intensify rainfall-driven floods in the Alps (Gobiet et al., 2014), our paleo-record demonstrates that natural cooling phases (e.g., the 17th-century Maunder Minimum) also elevated flood likelihood through delayed snowpack release. Conversely,, Peña and Schulte (2020) highlighted a correlation between colder-than-average periods and higher flood risk, corroborated by Blöschl et al., 2020 for the European floods. Wilhelm et al. (2022) conducted a comprehensive analysis of paleoflood records from the European Alps, aiming to clarify the uncertain impacts of climatic trends on flood frequency and magnitude. Their study demonstrated that a temperature increase of 0.5° - 1.2°C, whether driven by natural variability or anthropogenic factors, resulted in a significant reduction (25–50%) in the frequency of large floods, defined as those with a return period of 10 years or more. This trend, however, was not observed in records covering less than 200 years but remained persistent in longer paleoclimate datasets spanning from 200 to 9,000 years.

Precipitation variability, particularly multi-decadal oscillations in summer rainfall, further emerged as a critical flood driver. The Granger-causal link between precipitation and flood variability underscores the role of antecedent moisture conditions in preconditioning basins for extremes—a phenomenon documented in modern flood events (Barth et al., 2020) but rarely quantified over centennial scales (Schulte et al., 2019). Our results thus provide empirical support for incorporating multi-year hydrological memory into flood risk models (Merz et al., 2021).

5.4 Advancing Flood Prediction Through Bayesian Causal Networks

Taken together, these pathways suggest a cascade of influences: external forcings modulate atmospheric circulation (tier 1 → tier 2), which in turn governs both moisture delivery and thermal conditions (tier 2 → tier 3), ultimately shaping flood risk (tier 3 → tier 4). By enforcing physical constraints via blacklists and tiering, the causal graph avoids spurious feedback and yields an interpretable model that aligns with mechanistic understanding.

https://doi.org/10.5194/egusphere-2026-303
Preprint. Discussion started: 2 February 2026

These insights have important implications for paleoclimatic reconstructions and future projections. First, they reinforce the value of combining solar and volcanic proxies with circulation indices to improve hydroclimate reconstructions in complex terrain. Second, they provide a framework for data-driven attribution of past extreme events, offering a complementary approach to process-based climate models. Finally, the methodology can be generalized to other regions and forcing agents—such as greenhouse gases or land-use change—enabling a broader assessment of causal drivers in Earth system variability.

Bayesian causal networks offer a robust and adaptive framework (Pearl, 2019) for quantifying flood risks under various environmental scenarios. This approach is particularly effective in conditions where traditional predictive models may fall short due to complex and dynamic climatic influences.

The structural shifts identified between pre-industrial and industrial eras (notably the weakening of solar-forced pathways and the emergence of anthropogenic drivers) mirror patterns observed in global flood attribution studies (Mallakpour & Villarini, 2015). These findings underscore the need for epoch-specific flood models, as pre-industrial analogs may poorly represent modern risk landscapes dominated by greenhouse forcing and land-use change.

This comprehensive methodology enhances our understanding of the interplay between external forcings, climate components and their collective impact on flood risk. The discussion highlights key findings and explores their broader implications for flood management and climate adaptation strategies, emphasizing the importance of integrating global climate drivers and regional responses into predictive models (Wilby & Harris, 2006; Kundzewicz et al., 2013).

While our study advances paleoflood attribution, key limitations persist. Proxy chronological uncertainties (±20 years) may have attenuated high-frequency signals, masking sub-decadal flood triggers like convective storms (Wilhelm et al., 2022). Future work aims to refine chronological resolution, integrate additional proxy and data records as glaciers, soil-moisture, hydrologic management, and explore machine-learning-enhanced causal inference for improved robustness.

6 Conclusions

This work introduces a novel causal inference framework for climate proxy time series, combining the PC algorithm and Granger causality to reveal robust cause–effect relationships in the climate system. By conditioning on confounding influences, our methods substantially reduce spurious linkages and highlight true drivers of variability. Key contributions and findings include:

- **Innovative Methodology:** We demonstrate for the first time (to our knowledge) that constraint-based causal inference algorithms can be effectively applied to networks of paleoclimate proxy series. This represents an innovative advance over standard correlation-based reconstructions, echoing recent calls to leverage “novel data-driven causal methods” in Earth sciences.
- **Detection of Causal Links:** The analysis recovers known teleconnections (e.g. between distant proxy records linked by atmospheric circulation) and suggests previously undetected indirect pathways. These results emphasize the

https://doi.org/10.5194/egusphere-2026-303
Preprint. Discussion started: 2 February 2026

importance of multivariate causal inference in isolating direct influences, as the PC algorithm "unveils all spurious links".

- **Model Evaluation Potential:** By producing a causal fingerprint of the proxy network, our framework provides a new diagnostic that can inform climate model evaluation. Similar causal network approaches have been shown to identify model–data mismatches and constrain projection uncertainties more effectively than traditional metrics. In this way, our results suggest a promising avenue for using proxy-based causality to validate and improve climate simulations.
- **Broader Impact:** Ultimately, our study illustrates the promise of the "causal revolution" in climate. Observational causal inference methods, sensibly applied, can offer deeper insights into climate dynamics than correlation analysis alone. The causal networks we infer from proxy data not only advance our understanding of past climate drivers but also lay the groundwork for more reliable predictions and attributions in a changing climate.

Solar-driven atmospheric modes have significant implications for understanding climate dynamics and extreme weather events. Here are some key points derived from the paper:

- **Influence on Atmospheric Variability:** Total Solar Irradiance (TSI) is identified as a primary driver of atmospheric variability, particularly influencing the leading mode of atmospheric variability (EOF1). This relationship suggests that solar cycles can significantly affect large-scale circulation patterns, which are crucial for understanding climate dynamics.
- **Impact on Flood Dynamics:** The study highlights that solar variability can modulate flood dynamics in sensitive regions like the European Alps. The findings indicate that external solar forcing has historically influenced alpine flood patterns through changes in summer atmospheric circulation. This connection is particularly strong in the preindustrial era, suggesting that solar activity played a more dominant role in shaping hydroclimatic extremes before modern climate influences took over-
- **Causal Attribution of Flood Variability:** The research provides a robust causal attribution framework that links solar activity to flood variability. By employing a constraint-based causal inference approach, the study advances the understanding of how solar-driven atmospheric modes can lead to extreme flood events, thereby contributing to climate attribution.
- **Shifts in Climate Drivers:** The study indicates that the influence of solar-driven atmospheric modes on flood risk has weakened under modern anthropogenic forcing. This shift suggests that while solar activity was a significant driver of hydroclimatic extremes in the past, contemporary climate change factors are now more influential, altering the dynamics of flood risk in alpine.
- **Methodological Contributions:** The research introduces a novel methodological framework for applying causal discovery techniques to paleoclimate data. This approach not only enhances the understanding of natural versus anthropogenic influences on extreme events but also provides a reproducible template for future studies in climate.

https://doi.org/10.5194/egusphere-2026-303
Preprint. Discussion started: 2 February 2026

In summary, The innovative approach clarifies the key causal message of our work: that proxy time series contain rich causal information which can be extracted through multivariate inference, opening new perspectives for Earth system science. Solar-driven atmospheric modes have important implications for understanding climate variability and flood dynamics, particularly in the context of natural climate variability. The findings underscore the importance of considering solar influences in climate models and risk assessments.

Code, data, or code and data availability

The link to the code and data availability in Supplement link.

Supplement link

The link to the supplement will be included by Copernicus, if applicable.

Author contributions

JCPR and LS planned the research, LS and FC arrange the sedimentary data, JCPR and JR ran the causal inference model, JCPR, LS, JR and EM analysed the data, JCPR and LS wrote the manuscript draft, and all authors reviewed and edited the manuscript.

Competing interests

The contact author has declared that neither of the authors has any competing interests.

Disclaimer

Publisher's note: Copernicus Publications remains neutral with regard to jurisdictional claims made in the text, published maps, institutional affiliations, or any other geographical representation in this paper. The authors bear the ultimate responsibility for providing appropriate place names. Views expressed in the text are those of the authors and do not necessarily reflect the views of the publisher.

Acknowledgements

The authors want to thank the CESM1(CAM5), Last Millennium Ensemble Community Project, NSF/CISL/Yellowstone, DOE INCITE program, the Office of Biological and Environmental Research (BER), and NOAA which provided the 20 Century Reanalysis dataset, the EMULATE project, and the CESM-LME.

https://doi.org/10.5194/egusphere-2026-303
Preprint. Discussion started: 2 February 2026

Financial support

The work of the Fluvalps-PaleoRisk Research Group (2021 SGR 01106) was funded by the Spanish Ministry of Science, Innovation and Universities (PID2023 - 148210OTC - I00) and ICREA Program (ICREA Academia of Generalitat de Catalunya), and supported by the PAGES Flood Working Group.

Review statement

The review statement will be added by Copernicus Publications listing the handling editor as well as all contributing referees according to their status anonymous or identified.

References

Barth, N.A., Larsen, M.C., & Smith, J.A: Assessment of antecedent moisture condition on flood frequency: An experimental study in Napa River Basin, CA. NOAA Technical Report, 2020.

Blöschl, G., Hall, J., Parajka, J., Perdigão, R.A. P., Merz, B., Arheimer, B., Aronica, G.T., Bilibashi, A., Bonacci, O., Borga, M., Čanjevac, I., Castellarin, A., Chirico, G.B., Claps, P., Fiala, K., Frolova, N., Gorbachova, L., Gül, A., Hannaford, J., Harrigan, S., Kireeva, M., Kiss, A., Kjeldsen, T.R., Kohnová, S., Koskela, J.J., Ledvinka, O., Macdonald, N., Mavrova-Guirguinova, M., Mediero, L., Merz, R., Molnar, P., Montanari, A., Murphy, C., Osuch, M., Ovcharuk, V., Radevski, I., Rogger, M., Salinas, J.L., Sauquet, E., Šraj, M., Szolgay, J., Viglione, A., Volpi, E., Wilson, D., Zaimi, K., & Živković, N.: Current European flood-rich period exceptional compared with past 500 years. Nature 583, 560–56,. https://doi.org/10.1038/s41586-020-2478-3, 2020

Brönnimann, S., Krämer, D., & Pfister, C.: Tambora and the "Year Without a Summer" of 1816: A perspective on Earth and human systems science. Geographica Bernensia G92, 1–48, https://doi.org/10.4480/GB2019.G92.01, 2019.

Büntgen, U., Frank, D.C., Nievergelt, D., & Esper, J.: Summer Temperature Variations in the European Alps, a.d.755–2004. J. Clim. 19, 5606–5623, https://doi.org/10.1175/JCLI3917.1, 2006.

Büntgen, U., Tegel, W., Nicolussi, K., McCormick, M., Frank, D., Trouet, V., Kaplan, J.O., Herzig, F., Heussner, K.-U., Wanner, H., Luterbacher, J., & Esper, J.: 2500 years of European climate variability and human susceptibility. Science 331, 578-582, https://doi.org/10.1126/science.1197175, 2011

Büntgen, U., Arseneault, D., Boucher, É., Churakova (Sidorova), O.V., Gennaretti, F., Crivellaro, A., Hughes, M.K., Kirdyanov, A.V., Klippel, L., Krusic, P.J., Linderholm, H.W., Ljungqvist, F.C., Ludescher, J., McCormick, M., Myglan, V.S., Nicolussi, K., Piermattei, A., Oppenheimer, C., Reinig, F., Sigl, M., Vaganov, E.A. & Esper, J..: Prominent role of volcanism in Common Era climate variability and human history. *Dendrochronologia* 64, 125757, https://doi.org/10.1016/j.dendro.2020.125757, 2020

Carvalho O., Di Capua, G., Borchert, L.F., Donner, R. V., Donner, R. V.: Causal relationships and predictability of the summer East Atlantic teleconnection. Weather and Climate Dynamics. 5. 1561-1578, https://doi.org/10.5194/wcd-5-1561-2024, 2024

https://doi.org/10.5194/egusphere-2026-303
Preprint. Discussion started: 2 February 2026

Folland, C. K., Knight, J., Linderholm, H.W. , Fereday, D. , Ineson, S., Hurrell, J.W.: The summer North Atlantic oscillation: Past, present, and future. *J. Clim.* 22, 1082-1103, https://doi.org/10.1175/2008JCLI2459.1, 2009.

Gao, C., Robock, A., Ammann, C.: Volcanic forcing of climate over the past 1500 years: An improved ice-core-based index for climate models. *J. Geophys. Res. Atmos.* 113, D23111, https://doi.org/10.1029/2008JD010239, 2008.

Gobiet, A., Kotlarski, S,. Beniston, M., Heinrich, G., Rajczak, J., Stoffel, M. 21st century climate change in the European Alps—A review. *Sci. Total Environ.* 493, 1138–1151, https://doi.org/10.1016/j.scitotenv.2013.07.050, 2014.

Granger, C.W.J.: Investigating causal relations by econometric models and cross-spectral methods. *Econometrica* 37, 424–438, https://doi.org/10.2307/1912791, 1969

Beer, J., Geller, M., Haigh, J.D., Lockwood, M., Matthes, K., Cubasch, U., Fleitmann, D., Harrison, G., Hood, L., Luterbacher, J., Meehl, G. A., Shindell, D., van Geel, B., White, W.: Solar Influences on Climate. *Rev. Geophys.* 48, RG4001, https://doi.org/10.1029/2009RG000282, 2010.

Hirschi, M., Seneviratne, S. I., Schär, C.: Seasonal Variations in Terrestrial Water Storage for Major Midlatitude River Basins. J. Hydrometeor., 7, 39–60, https://doi.org/10.1175/JHM480.1, 2006.

Horton, P., Schaefli, B., Mezghani, A., Hingray, B., Musy, A.: Assessment of climate change impacts on alpine discharge regimes with climate model uncertainty. *Hydrol. Process.* 20, 2091–2109, https://doi.org/10.1002/hyp.6197, 2006.

Hurrell, J.W.: Decadal trends in the North Atlantic Oscillation: regional temperatures and precipitation. *Science* 269, 676–679, https://doi.org/10.1126/science.269.5224.676, 1995

IPCC. Climate Change 2021: The Physical Science Basis. *Cambridge Univ. Press* (2021). https://www.ipcc.ch/report/ar6/wg1/

Kalisch, M. & Bühlmann, P.: Estimating high-dimensional directed acyclic graphs with the PC-algorithm. *J. Mach. Learn. Res.* 8, 613–636, https://doi.org/10.48550/arXiv.math/0510436, 2007

Knudsen, M. F., Riisager, P. , Jacobsen, B. H., Muscheler, R., Snowball, I., Seidenkrantz, M.S.: Taking the pulse of the Sun during the Holocene by joint analysis of 14C and 10Be, Geophys. Res. Lett., 36, L16701, https://doi.org/10.1029/2009GL039439, 2009.

Kretschmer, M., Coumou, D., Donges, J. F. Runge, J.: Using causal effect networks to analyze different Arctic drivers of midlatitude winter circulation. *J. Clim.* 29, 4069–4081, https://doi.org/10.1175/JCLI-D-15-0654.1, 2016

Kretschmer, M., Adams, S. V., Arribas, A., Prudden, R., Robinson, N., Saggioro, E., Shepherd, T. G.: Quantifying Causal Pathways of Teleconnections. Bulletin of the American Meteorological Society. 102, https://doi.org/10.1175/BAMS-D-20-0117.1, 2021.

Kundzewicz, Z. W., Kanae, S., Seneviratne, S. I., Handmer, J., Nicholls, N., Peduzzi, P., Mechler, R., Bouwer, L. M., Arnell, N., Mach, K., Muir-Wood, R., Brakenridge, G. R., Kron, W., Benito, G., Honda, Y., Takahashi, K., Sherstyukov, B.: Flood risk and climate change: global and regional perspectives. Hydrological Sciences Journal, 59(1), 1–28, https://doi.org/10.1080/02626667.2013.857411, 2013.

https://doi.org/10.5194/egusphere-2026-303
Preprint. Discussion started: 2 February 2026

Laternser, M. & Schneebeli, M.: Long-term snow climate trends of the Swiss Alps (1931–99). *Int. J. Climatol.* 23, 733–750, https://doi.org/10.1002/joc.912, 2003.

Lean, J. L., Coddington, O., Marchenko, S. V., DeLand, M. T.: A new model of solar ultraviolet irradiance variability with 0.1–0.5 nm spectral resolution. Earth and Space Science, 9, e2021EA002211, https://doi. org/10.1029/2021EA002211, 2022.

Luterbacher, J , Werner, J P , Smerdon, J E , Fernández-Donado, L , González-Rouco, F J , Barriopedro, D , Ljungqvist, F C, Büntgen, U , Zorita, E , Wagner, S , Esper, J , McCarroll, D , Toreti, A , Frank, D , Jungclaus, J H , Barriendos, M , Bertolin, C , Bothe, O , Brázdil, R , Camuffo, D , Dobrovolný, P , Gagen, M , García-Bustamante, E , Ge, Q , Gómez-Navarro, J J , Guiot, J , Hao, Z , Hegerl, G C , Holmgren, K , Klimenko, V V , Martín-Chivelet, J , Pfister, C , Roberts, N , Schindler, A , Schurer, A , Solomina, O , von Gunten, L , Wahl, E , Wanner, H , Wetter, O , Xoplaki, E , Yuan, N , Zanchettin, D , Zhang, H , Zerefos, C.: European summer temperatures since Roman times. Environ. Res. Lett. 11 024001, DOI 10.1088/1748-9326/11/2/024001, 2016.

Mallakpour, I. & Villarini, G.: The changing nature of flooding across the central United States. *Nat. Clim. Chang.* 5, 250–254, https://doi.org/10.1038/nclimate2516, 2015.

Martín-Chivelet, J., Belén Muñoz-García, M. , Lawrence Edwards, R., Turrero, M.J. Ortega, Ana I.: Land surface temperature changes in Northern Iberia since 4000yrBP, based on δ13C of speleothems, Global and Planetary Change,Volume 77, Issues 1–2, https://doi.org/10.1016/j.gloplacha.2011.02.002, 2011.

Merz, B., Blöschl, G., Vorogushyn, S., Dottori, F., Aerts, J. C. J. H., Bates, P., Bertola, M., Kemter, M., Kreibich, H., Lall, U., Macdonald, E.: Causes, impacts and patterns of disastrous river floods. Nat Rev Earth Environ 2, 592–609, https://doi.org/10.1038/s43017-021-00195-3, 2021.

Moffa-Sánchez, P., Moreno-Chamarro, E., Reynolds, D.J., Ortega, P., Cunningham, L., Swingedouw, D., Amrhein, D.E., Halfar, J., Jonkers, L., Jungclaus, J.H., Perner, K., Wanamaker, A. and Yeager, S.: Variability in the Northern North Atlantic and Arctic Oceans Across the Last Two Millennia: A Review. Palaeoceanography and Paleoclimatology, 34: 1399-1436, https://doi.org/10.1029/2018PA003508, 2019.

Pearl, J.: *Causality: Models, Reasoning, and Inference*. Cambridge Univ. Press, 2000.

Pearl, J.: The seven tools of causal inference, with reflections on machine learning. *Commun. ACM* 62, 54–60, https://doi.org/10.1145/3241036, 2019.

Peña, J.C. & Schulte, L:. Simulated and reconstructed atmospheric variability and their relation with large pre-industrial summer floods in the Hasli-Aare catchment (Swiss Alps) since 1300 CE. *Glob. Planet. Change* 184, 103052, https://doi.org/10.1016/j.gloplacha.2020.103191, 2020.

Peña, J. C., Schulte, L., Badoux, A., Barriendos, M., and Barrera-Escoda, A.: Influence of solar forcing, climate variability and modes of low-frequency atmospheric variability on summer floods in Switzerland. *Hydrol. Earth Syst. Sci.* 19, 3807–3827, https://doi.org/10.5194/hess-19-3807-2015, 2015.

Peters, J., Janzing, D., Schölkopf, B.: Elements of Causal Inference. MIT Press, 2017.

Robock, A.: Volcanic eruptions and climate. Rev. Geophys., 38, 191-219, **https://doi.org/10.1029/1998RG000054**, 2000.

https://doi.org/10.5194/egusphere-2026-303
Preprint. Discussion started: 2 February 2026

Runge, J., Bathiany, S., Bollt, E. et al.: Inferring causation from time series in Earth system sciences. *Nat. Commun.* 10, 2553, https://doi.org/10.1038/s41467-019-10105-3, 2019.

Runge, J., Nowack, P., Kretschmer, M., Flaxman, S., Sejdinovic, D.: Detecting and quantifying causal associations in large nonlinear time series datasets. *Sci. Adv.* 5, eaau4996, https://doi.org/10.1126/sciadv.aau4996, 2019.

Schulte, L., Julià, R., Oliva, M., Burjachs, F., Veit, H., & Carvalho, F.: Sensitivity of Alpine fluvial environments in the Swiss Alps to climate forcing during the Late Holocene. Sediment Dynamics in Changing Environments. IAHS Publ. 325, 367-374 (2008).

Schulte, L.; Schillereff, D.; Santisteban, J.I.: Pluridisciplinary analysis and multi-archive reconstruction of paleofloods: societal demand, challenges and progress. Global and Planetary Change 177, 225-238, https://doi.org/10.1016/j.gloplacha.2019.03.019, 2019.

Schulte, L., Peña, J. C., Carvalho, F., Schmidt, T., Julià, R., Llorca, J., and Veit, H.: A 2600-year history of floods in the Bernese Alps, Switzerland: frequencies, mechanisms and climate forcing, Hydrol. Earth Syst. Sci., 19, 3047–3072, https://doi.org/10.5194/hess-19-3047-2015, 2015.

Schulte, L.; Oliver Wetter, O.; Wilhelm, B.; Peña, J.C.; Amann, B.; Wirth S.B.; Carvalho, F.; Gómez-Bolea, A.: Integration of multi-archive datasets towards the development of a four-dimensional paleoflood model in alpine catchments. Global and Planetary Change 180, 66-88, https://doi.org/10.1016/j.gloplacha.2019.05.011, 2019.

Scutari, M.: Learning Bayesian Networks with the bnlearn R Package. *J. Stat. Softw.* 35, 1–22, https://doi.org/10.18637/jss.v035.i03, 2010.

Schneider, D. P., C. M. Ammann, B. L. Otto-Bliesner, and D. S. Kaufman.: Climate response to large, high-latitude and low-latitude volcanic eruptions in the Community Climate System Model, J. Geophys. Res., 114, D15101, https://doi.org/10.1029/2008JD011222, 2009.

Shruti Verma, Bhatla, R., Shahi, N.K., Mall, R.K.: Regional modulating behaviour of Indian summer monsoon rainfall in context of spatio-temporal variation of drought and flood events. *Atmos. Res.* 274, 106201, https://doi.org/10.1016/j.atmosres.2022.106201, 2022.

Sigl, M., Winstrup, M., McConnell, J. et al.: Timing and climate forcing of volcanic eruptions for the past 2,500 years. *Nature* 523, 543–549, https://doi.org/10.1038/nature14565, 2015.

Silini, R., Tirabassi, G., Barreiro, M., Ferranti, L., Masoller, C.: Assessing causal dependencies in climatic indices. *Clim. Dyn.* 61, 79–89, https://doi.org/10.1007/s00382-022-06562-0, 2023.

Spirtes, P. Glymour, C., Scheines, R.: *Causation, Prediction, and Search*. MIT Press, 2000.

Steinhilber, F. , Beer, J., Fröhlich, C.; Total solar irradiance during the Holocene. *Geophys. Res. Lett.* 36, L19704, https://doi.org/10.1029/2009GL040142, 2009.

Stoffel, M., Khodri, M., Corona, C. Guillet, S., Poulain, V., Bekki, S., Guiot, J., Luckman, B.H., Oppenheimer, C., Lebas, N., Beniston, M., Masson-Delmotte, V.: Estimates of volcanic-induced cooling in the Northern Hemisphere over the past 1,500 years. *Nat. Geosci.* 8, 784–788, https://doi.org/10.1038/ngeo2526, 2015.

Su, J., Chen, D., Zheng, D. Su, Y., Li, X.: The insight of why: Causal inference in Earth system science. *Sci. China Earth Sci.* 66, 1415–1430, https://doi.org/10.1007/s11430-023-1148-7, 2023.

Toohey, M., Sigl, M.: Volcanic stratospheric sulphur injections and aerosol optical depth from 500 BCE to 1900 CE. *Earth Syst. Sci. Data* 9, 809–831, https://doi.org/10.5194/essd-9-809-2017, 2017.

Wu, C. J. , Usoskin, I. G. , Krivova, N. , Kovaltsov, G. A. ,Baroni, M. , Bard, E. , Solanki, S. K.: Solar Activity Over Nine Millennia: A Consistent Multi-Proxy Reconstruction. *Astron. Astrophys.* 649, A141, https://doi.org/10.1002/grl.50361, 2018.

Viviroli, D., Dürr, H. Messerli, B., Meybeck, M., Weingartner, R.: Mountains of the world, water towers for humanity: Typology, mapping, and global significance. *Water Resour. Res.* 43, W07447, https://doi.org/10.1029/2006WR005653, 2007.

Wilby, R.L. & Harris, I.: A framework for assessing uncertainties in climate change impacts: Low-flow scenarios for the River Thames, UK. *Water Resour. Res.* 42, W02419, https://doi.org/10.1029/2005WR004065, 2006.

Wilhelm, B., W. Rapuc, Benjamin Amann, F. S. Anselmetti, F. Arnaud, J. Blanchet, A. Brauer, M. Czymzik, C. Giguet-Covex, A. Gilli, L. Glur, M. Grosjean, R. Irmler, M. Nicolle, P. Sabatier, T. Swierczynski, S. B. Wirth.: Impact of warmer climate periods on flood hazard in the European Alps. *Nat. Geosci.* 15, 118–123, https://doi.org/10.1038/s41561-021-00878-y, 2022.

Wirth, S. B., Glur, L., Gilli, A., Anselmetti, F. S.: Holocene flood frequency across the Central Alps - Solar forcing and evidence for variations in North Atlantic atmospheric circulation. *Quat. Sci. Rev.* 80, 112–128, https://doi.org/10.1016/j.quascirev.2013.09.002, 2013.

Xiang, G., Wang, H., Yu, K., Guo, X., Cao, F., Song, Y:. Bootstrap-Based Layerwise Refining for Causal Structure Learning. *IEEE Trans. Artif. Intell.* 5, 2708–2722, https://doi.org/10.1109/TAI.2023.10168818, 2023.

Zanchettin, D., Rubino, A., Traverso, P., Tomasino, M.: Impact of variations in solar activity on hydrological decadal patterns in northern Italy. *J. Geophys. Res. Atmos.* 113, D12102, https://doi.org/10.1029/2007JD009157, 2008.

Links to the different data are as follows:

CESM Paleoclimate Working Group at NCAR. Last Millennium Ensemble Project. Disponible en: https://www.cesm.ucar.edu/community-projects/lme. Latest access: September de 2025.

NOAA Physical Sciences Laboratory. Twentieth Century Reanalysis Project dataset. Disponible en: https://psl.noaa.gov/data/20thC_Rean/. Latest access: September de 2025

Luterbacher, J. et al. Reconstruction of Sea Level Pressure fields over the eastern North Atlantic and Europe back to 1500 AD. Disponible in: https://www.ncdc.noaa.gov/paleo-search/study/6366. Latest access: September de 2025.

Ansell, T. J. et al. Reconstruction of Sea Level Pressure fields of EMULATE project. Disponible in: https://www.metoffice.gov.uk/hadobs/emslp/data/download.html. Latest access: September de 2025.

Büntgen, U. et al. Summer temperature for the Alps back to 1300 AD. Disponible en: https://www.ncdc.noaa.gov/paleo-search/study/5739. Latest access: September de 2025.

Steinhilber, F. et al. Total solar irradiance (TSI). Supplementary data available in: https://agupubs.onlinelibrary.wiley.com/action/downloadSupplement?doi=10.1029%2F2009GL040142&file=grl26405-sup-0002-ds01.txt. Latest access: September de 2025.

https://doi.org/10.5194/egusphere-2026-303
Preprint. Discussion started: 2 February 2026

Gao, C. et al. Volcanic Eruptions for the Northern Hemisphere. http://climate.envsci.rutgers.edu/IVI2/. Latest access: September de 2025.